The influence of time integrator on contact/impact problems using the positional finite element method

Darcy Hannah Falcão Rangel Moreira[1], Péricles Rafael Pavão Carvalho[1], Rodolfo André Kuche Sanches[1]

[1]*Structural Engineering Department, São Carlos School of Engineering, University of São Paulo*
Av. Trabalhador Saocarlense, 400, São Carlos, São Paulo, Brazil
darcyhannah@usp.br, periclescarvalho@usp.br, rodolfo.sanches@usp.br

Abstract. The dynamic structural problems involving contact/impact are strongly nonlinear, and can lead to spurious numerical oscillations, generating unsatisfactory results or even convergence problems depending on the applied temporal and spatial discretization techniques. The use of Newmark method with traditional parameters is proven to be inefficient in this case, making necessary the application of specialized time integration techniques. Some authors propose alternative values for the Newmark parameters to circumvent this problem, introducing a numerical damping in the system, and reducing artificially the high frequency oscillations. However, this strategy is highly sensitive to the time discretization, decreasing the accuracy of the results when the time steps are not sufficiently refined. As an alternative, one can employ the alpha-generalized time integration method, which allows the control of numerical dissipation by using appropriate parameters. In this work, we apply different combinations of said parameters, including the ones which reproduce the Newmark method and its variations, in order to analyze the numerical stability of two-dimensional impact problems. The applied computational framework is the positional finite element method, which is characterized by using positions as nodal parameters, instead of displacements, and naturally considering geometrical nonlinearities in its formulation. The applied constitutive model is the Neo-Hookean, for large strain. For the numerical implementation of structural contact, we make use of a node-to-segment model with Lagrange multipliers, employing a contact detection algorithm based on the intersection of trajectories. Finally, a representative numerical example is proposed with different time integration techniques. The results indicate that the adequate choice of alpha-generalized parameters can lead to quite significant improvements to the numerical stability when compared to the traditional Newmark method and its modifications.

Keywords: Time integrator, Structural contact, Positional Finite Element Method

1 Introduction

The Finite Element Method has been applied to nonlinear problems for a significant time, as can be seen in works such as Hughes and Carnoy [1], with shell elements, Schulz and Filippou [2] with beam elements in Lagrangian formulation and Crisfield [3] with solid elements. Seeking an alternative approach, Coda [4] introduces the positional finite element method, which employs degrees of freedom in positions, instead of traditional displacements. This approach has been successfully applied to static and dynamic problems with trusses elements [5] and shells [6] in several applications, including structural contact cases [7, 8]. This formulation is more compact, as can be seen in Avancini and Sanches [9], making its writing simpler and more straightforward. Furthermore, the position-based formulation is naturally and truly isoparametric, since its nodal parameters (problem unknowns) are the current coordinates of the solid.

The contact between deformable solids can be numerically modeled in two steps: detection of the intersection point and imposition of non-penetration conditions, with the solution procedure being directly affected by the discretization technique. One of these techniques is the node-to-node (NTN), used by Mashayekhi et al. [10], characterized by having only a nodal base and requiring an appropriate coincidence of the meshes, therefore unsuitable for general large displacement problems. By means of the node-to-segment (NTS) scheme, or node-to-surface for 3 dimensions, introduced by Hughes et al. [11], it is possible to distinguish the contact interfaces

as slave-nodes (defined by nodes of the slave-body) and master-segments or surfaces (defined by the boundary elements on the master-body). Another alternative method is the segment-to-segment (STS), or surface-to-surface for 3 dimensions, found in Puso and Laursen [12], which proposes an approach with high precision in the contact constraints. For a more detailed discussion on these discretization methods, one can refer to Wriggers [13].

Regarding the contact modelling in dynamic analyses, there is a challenge in temporal integration due to the instabilities caused by high-frequency oscillations. In order to control the numerical dissipation and stabilize the results in these cases, integration methods such as the *alpha*-Generalized [14] can be used. Arnold and Bruls [15] studies the convergence of this integrator to constrained mechanical systems, and Siqueira [16] applies the method to the simulation of sliding connections with restrictions in the system movement. By changing its parameters, the *alpha*-Generalized method can also represent other temporal integrators, such as Newmark's [17] with its traditional parameters ($\gamma = 1/2$ and $\beta = 1/4$) or with those proposed by Hu [18] ($\gamma = 3/2$ and $\beta = 1$). The latter is also suitable for impact problems, introducing a numerical damping on the system which reduces the high-frequency oscillations. However, as can be seen in Carvalho [7], Hu's integrator is greatly sensitive to the time discretization, which can lead to inconsistent and inaccurate results.

In this work, we propose a comparative study between time integrator methods for a large displacement and large strain two-dimensional impact problem. The applied numerical framework is the Positional Finite Element Method, described briefly in the sections 2 and 3. For the contact model, discussed in section 4, we employ a node-to-segment discretization, with a detection strategy based on the intersection of trajectories, and imposition of constraints via the Lagrange multiplier method. The *alpha*-Generalized method, described in section 5, is applied as a general time integrator, and different choices of parameters are discussed in the numerical example shown in section 6, including the one corresponding to Hu's integrator [18], and the ones proposed originally by Chung and Hulbert [14] for dealing with the high-frequency oscillations. The results and conclusions of the analysis are discussed in section 7.

2 Solid mechanics

The state of mechanical equilibrium occurs when the variation in the total mechanical energy functional (Π) is null, which translates the principle of stationarity. In this work, the functional Π is composed by the sum of the potential energies of the external forces ($\mathbb{P}$), strain ($\mathbb{U}$), kinetic ($\mathbb{K}$) and contact ($\mathbb{C}$). The latter is discussed in more details on section 4 . For the remaining parts, the equilibrium is expressed in variational form as

$$\delta\Pi = \underbrace{-\int_{\Gamma_0} \mathbf{q}\cdot\delta\mathbf{y}\, d\Gamma_0 - \int_{\Omega_0} \mathbf{b}\cdot\delta\mathbf{y}\, d\Omega_0}_{\delta\mathbb{P}} + \underbrace{\int_{\Omega_0} \mathbf{S}:\delta\mathbf{E}\, d\Omega_0}_{\delta\mathbb{U}} + \underbrace{\frac{1}{2}\int_{\Omega_0} \rho_0\ddot{\mathbf{y}}\cdot\delta\mathbf{y}\, d\Omega_0}_{\delta\mathbb{K}} = 0, \tag{1}$$

where $\mathbf{q}$ and $\mathbf{b}$ denote the conservative forces distributed along the initial surface Γ_0 and the initial volume Ω_0, respectively, ρ_0 is the initial density of the material, $\mathbf{y}$ denotes the position vectors, $\mathbf{S}$ is the second Piola-Kirchhoff stress, and $\mathbf{E}$ is the Green-Lagrange strain, defined as

$$\mathbf{E} = \frac{1}{2}(\mathbf{A}^T\cdot\mathbf{A} - \mathbf{I}), \tag{2}$$

with $\mathbf{A}$ denoting the deformation gradient, and $\mathbf{I}$ the identity tensor.

The second Piola-Kirchhoff stress is the energetic conjugate of $\mathbf{E}$, and can be defined as $\mathbf{S} = \partial u_e/\partial\mathbf{E}$, in which u_e is the strain energy density, defined by the constitutive model of the material. In this work, we apply an hyperelastic model of Neo-Hookean type, written as:

$$u_e = \mu(\mathrm{tr}\,\mathbf{E} - ln\, J) + \frac{\Lambda}{2}\,(ln\, J)^2, \tag{3}$$

where Λ and μ are the Lamé constants of the material, $J = det(\mathbf{A})$ is the Jacobian, and tr $(\cdot)$ denotes the trace of a tensor, i.e. $\mathrm{tr}\,\mathbf{E} = \mathbf{E} : \mathbf{I}$.

3 Positional Finite Element Method

For the two-dimensional finite element implementation, we apply 10-node triangular elements (T10) with cubic polynomials as shape functions. For each element, the positions and accelerations can be written, respectively, as $\mathbf{y} = \varphi^\alpha \mathbf{y}^\alpha$ and $\ddot{\mathbf{y}} = \varphi^\alpha \ddot{\mathbf{y}}^\alpha$, where, for each node α, $\mathbf{y}^\alpha$ is the position, $\ddot{\mathbf{y}}^\alpha$ is the acceleration, and φ^α is the shape function. From the Galerkin method, one can also write $\delta\mathbf{y} = \varphi^\alpha \delta\mathbf{y}^\alpha$. Then, by using the arbitrarity of $\delta\mathbf{y}^\alpha$, the equilibrium equation (1) can be expressed as

$$\mathbf{f}^{int} + \mathbf{f}^{iner} - \mathbf{f}^{ext} = \mathbf{0}, \tag{4}$$

where $\mathbf{f}^{int}$, $\mathbf{f}^{iner}$ and $\mathbf{f}^{ext}$ represent the internal, inertial and external forces, respectively, and can be written, for each node α, as

$$\mathbf{f}_\alpha^{int} = \int_{\Omega_0} \mathbf{S} : \frac{\partial \mathbf{E}}{\partial \mathbf{y}^\alpha}\, d\Omega_0, \quad \mathbf{f}_\alpha^{iner} = \frac{1}{2}\int_{\Omega_0} \rho_0 \varphi^\alpha \varphi^\beta \ddot{\mathbf{y}}^\beta\, d\Omega_0, \quad \mathbf{f}_\alpha^{ext} = \int_{\Gamma_0} \varphi^\alpha \mathbf{q}\, d\Gamma_0 + \int_{\Omega_0} \varphi^\alpha \mathbf{b}\, d\Omega_0. \tag{5}$$

The non-linear Equation (4) can be solved by the Newton-Raphson method. For further details regarding the Positional Finite Element Method, one can refer to Coda [19].

4 Contact model

For the numerical implementation of contact, we adopt the node-to-segment strategy, in which the contact interfaces are treated in pairs, one discretized by nodes, called slave-nodes, and other discretized by curved line elements, called master-segments.

4.1 Contact detection

The contact detection is based on the intersection of slave-node and master-segment trajectories. The trajectories are mapped through a 'dimensionless time' parameter θ, going from 0 (previous step) to 1 (current step). The position of a slave-node between the steps can be approximated in terms of θ by the linear interpolation

$$\mathbf{y}^N(\theta) = \theta \mathbf{y}_{s+1}^N + (1-\theta)\mathbf{y}_s^N \tag{6}$$

where $\mathbf{y}_{s+1}^N$ and $\mathbf{y}_s^N$ represent the positions of the node on the current and previous time step, respectively.

For the master-segment, the positions are determined by the finite element approximation $\mathbf{y}(\xi) = \varphi^\alpha(\xi)\mathbf{y}^\alpha$, where φ^α is the shape function of each node α in the curved line element, parametrized by the dimensionless coordinate ξ, with values from -1 to 1. Therefore, for an arbitrary dimensionless time θ, the positions on a master-segment can be interpolated by the equation

$$\mathbf{y}^S(\xi,\theta) = \varphi^\alpha(\xi)\left[\theta \mathbf{y}_{s+1}^\alpha + (1-\theta)\mathbf{y}_s^\alpha\right]. \tag{7}$$

The intersection of trajectories is calculated by the equation $\mathbf{y}^N(\theta) = \mathbf{y}^S(\xi,\theta)$, which, for the two dimensional case, leads to a non-linear system of two equations with two unknowns (ξ and θ), solved in this work by the Newton-Raphson method. The contact between a slave-node and a master-segment is activated if the solution to this system is valid, i.e. if the resulting θ is a value between 0 and 1, and ξ is a value between -1 and 1. Furthermore, it is necessary that the slave-node has penetrated the master structure, i.e. the normal projection (g_n) of the slave-node on the master-segment is less than or equal to zero on the current step:

$$g_n = \left[\mathbf{y}_{s+1}^N - \varphi^\alpha(\xi)\mathbf{y}_{s+1}^\alpha\right] \cdot \mathbf{n}(\xi) \leq 0 \tag{8}$$

where $\mathbf{n}$ is the unitary normal vector of the master-segment on the contact point ξ, directed to outside of the solid domain.

4.2 Imposition of contact constraints

After the contact identification, it is necessary to activate the contact restriction for the slave-nodes and master-segments involved. To apply the impenetrability condition in the frictionless case, one must add the constraint $g_n = 0$ to the system. In the present work, this condition is imposed by the Lagrange multiplier method. Through this technique, for each contact pair, an additional parcel $\mathbb{C}$ is added to the mechanical energy functional, expressed as $\mathbb{C} = \lambda g_n$, where λ is a new nodal parameter of the system called Lagrange multiplier. Then, the variation $\delta\mathbb{C} = g_n\delta\lambda + \lambda\delta g_n$ is added to the equilibrium equation (1). From eq. (8), one can write

$$\delta\mathbb{C} = g_n\delta\lambda + \lambda\mathbf{n}\delta\mathbf{y}^N - \lambda\varphi^\alpha\mathbf{n}\,\delta\mathbf{y}^\alpha + \lambda\left[\mathbf{y}^N - \varphi^\alpha\mathbf{y}^\alpha(\xi)\right]\cdot\frac{\partial\mathbf{n}}{\partial\mathbf{y}^\alpha}\,\delta\mathbf{y}^\alpha, \tag{9}$$

where the variables are taken on the current step. From the arbitrarity of $\delta\lambda$, $\delta\mathbf{y}^N$ and $\delta\mathbf{y}^\alpha$, new forces of contact are added to the equilibrium equation (4). For the slave-node, the contact force is expressed as

$$\mathbf{f}_N^{cont} = \lambda\mathbf{n}, \tag{10}$$

and for the master-segment, the contact force in each node α is expressed as

$$\mathbf{f}_\alpha^{cont} = -\lambda\varphi^\alpha\mathbf{n} + \lambda\left[\mathbf{y}^N - \varphi^\alpha\mathbf{y}^\alpha(\xi)\right]\cdot\frac{\partial\mathbf{n}}{\partial\mathbf{y}^\alpha}. \tag{11}$$

Furthermore, a new equation is added to the system, called non-penetration condition, which reads

$$g_n = \left[\mathbf{y}^N - \varphi^\alpha\mathbf{y}^\alpha\right]\cdot\mathbf{n}(\xi) = 0 \tag{12}$$

It is important to note that λ has the physical meaning of normal contact force, as can be induced from eq. (10). Since the current model does not account for adhesion, it is expected that λ only assumes negative values (which correspond to compression forces). Therefore, the condition for contact deactivation is $\lambda \geq 0$.

5 Time integrator

One of the most commonly adopted time integrators for dynamic analyses of structural problems is the Newmark-β method, which derives from the equations

$$\mathbf{y}_{s+1} = \mathbf{y}_s + \dot{\mathbf{y}}_s\Delta t + \left[\left(\frac{1}{2} - \beta\right)\ddot{\mathbf{y}}_s + \beta\ddot{\mathbf{y}}_{s+1}\right]\Delta t^2 \tag{13}$$

$$\dot{\mathbf{y}}_{s+1} = \dot{\mathbf{y}}_s + (1-\gamma)\Delta t\ddot{\mathbf{y}}_s + \gamma\Delta t\ddot{\mathbf{y}}_{s+1} \tag{14}$$

where the indexes $(\cdot)_{s+1}$ and $(\cdot)_s$ refer to the current and previous time steps, respectively, Δt is the time interval between time steps, and γ and β are the Newmark parameters, controlling the stability and precision of the method. The traditional values for structural analyses are $\gamma = 1/2$ and $\beta = 1/4$, which result in an unconditionally stable method with second-order accuracy. However, these values are not suitable for high frequency impact problems. As an alternative, Hu [18] proposed the parameters $\gamma = 3/2$ and $\beta = 1$, which eliminates the high-frequency oscillations by introducing a numerical damping on the system.

A more general time integrator, applied in this work, is the *alpha*-generalized method, characterized by performing the integration in an intermediate time instant '$s + 1 - \alpha$', where the variables are calculated in terms of previous and current values by the linear interpolation $(\cdot)_{s+1-\alpha} = (1-\alpha)(\cdot)_{s+1} + \alpha(\cdot)_s$. In the equilibrium equation, we take $\alpha = \alpha_m$ for the inertial forces, and $\alpha = \alpha_f$ for the remaining parcels, including the contact forces, resulting in the following equation:

$$(1-\alpha_f)(\mathbf{f}_{s+1}^{int} + \mathbf{f}_{s+1}^{cont} - \mathbf{f}_{s+1}^{ext}) + \alpha_f(\mathbf{f}_s^{int} + \mathbf{f}_s^{cont} - \mathbf{f}_s^{ext}) + (1-\alpha_m)\mathbf{f}_{s+1}^{iner} + \alpha_m\mathbf{f}_s^{iner} = \mathbf{0} \tag{15}$$

For the identification of velocities and accelerations on the current step, the Newmark equations (13) and (14) can still be used. Therefore, the time integrator is defined by four parameters: α_m, α_f, γ and β. We note that, by taking $\alpha_m = \alpha_f = 0$, the equilibrium equation is evaluated purely on the current time step, falling back to the Newmark integrator.

In order to guarantee consistency and stability for the *alpha*-generalized method, Chung and Hulbert [14] proposed the choice of parameters in terms of a spectral radius ρ_∞, following the equations

$$\alpha_m = \frac{2\rho_\infty - 1}{\rho_\infty + 1} \qquad \text{and} \qquad \alpha_f = \frac{\rho_\infty}{\rho_\infty + 1}, \tag{16}$$

and, in order to maximize the high-frequency dissipations and guarantee the second-order accuracy,

$$\gamma = \frac{1}{2} - \alpha_m + \alpha_f \qquad \text{and} \qquad \beta = \frac{1}{4}(1 - \alpha_m + \alpha_f)^2. \tag{17}$$

According to Chung and Hulbert [14], the spectral radius is a measure of numerical dissipation, defined in $[0, 1]$, with $\rho_\infty = 1$ corresponding to no dissipation, and smaller values corresponding to greater dissipation.

6 Numerical example: impact between two deformable bodies

The analysed example consists of a cylinder that, under the action of gravity, falls onto a rectangular prism of negligible self-weight. This problem is strongly nonlinear due to dynamic contact (impact), and its numerical solution is quite unstable. Both structures are considered deformable, with materials described using the Neo-Hookean hyperelastic model. The geometry and boundary conditions of the problem are indicated in Fig. 1(A). Taking advantage of the problem's symmetry, only half of the structures are discretized, and appropriate boundary conditions are applied to the symmetry axis. The density of the material is taken as $\rho = 0.25$ kg/m^3, and the Lamé constants are $\Lambda = 200$ N/m^2 and $\mu = 15$ N/m^2.

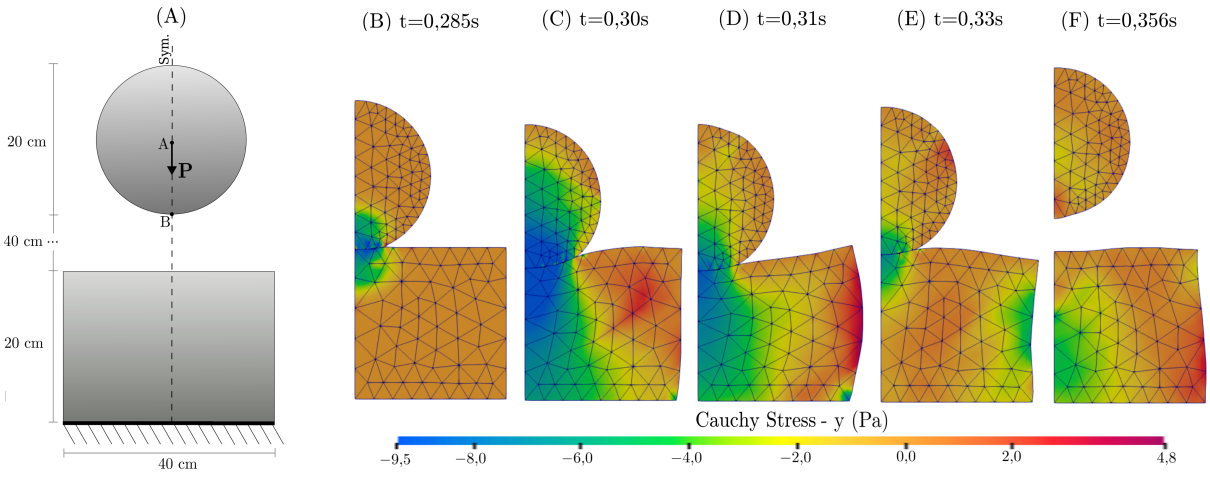

Figure 1. Problem geometry and boundary conditions (A) and Cauchy stress variation in the structure in its deformed configuration for different moments of the analysis (B), (C), (D), (E), (F), for $\rho_\infty = 0.1$.

Some simulations were performed with different values for the alpha-generalized integrator parameters and Δt. For the first analysis, the parameters are taken as $\alpha_f = 0$, $\alpha_m = 0$, $\gamma = 3/2$ and $\beta = 1$, and the time discretizations as $\Delta t = 1,875 \cdot 10^{-4}$s and $\Delta t = 5,85 \cdot 10^{-6}$s. It should be noted that, for these values, the alpha-Generalized method falls back to the Newmark integrator with the parameters suggested in Hu [18]. For the next analysis, we follow the proposal of Chung and Hulbert [14] and base the parameters on a spectral radius ρ_∞. Seeking an optimal dissipation of high-frequencies, two parameters are adopted: $\rho_\infty = 0.6$ and $\rho_\infty = 0.1$, with $\Delta t = 1{,}875 \cdot 10^{-3}$ s in both.

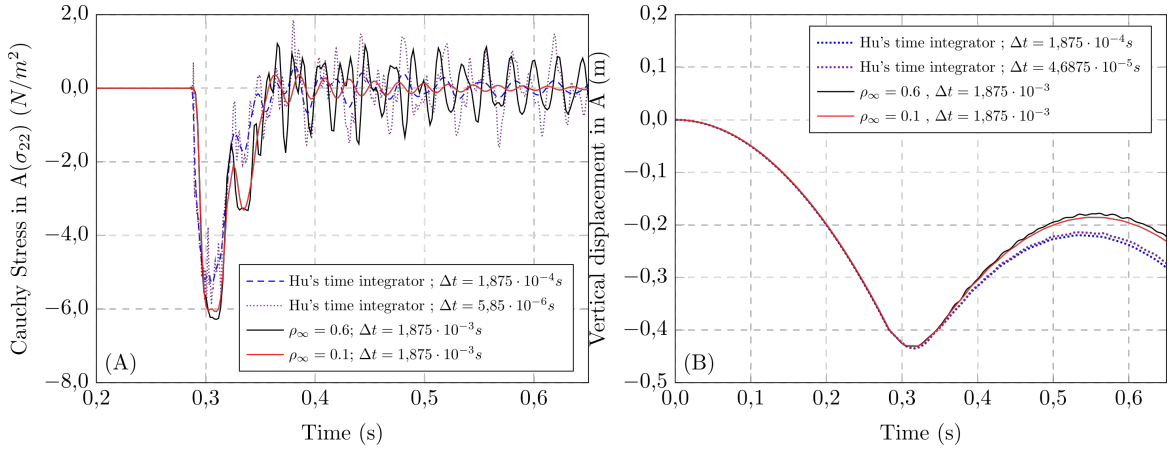

Figure 2. Normal Cauchy stress distribution in the vertical direction at B (A) and vertical displacement at A (B) versus time for different simulations

Figure 1(B)-(F) illustrates the deformed configurations for different time steps in the case with $\rho_\infty = 0.1$, displaying the vertical Cauchy Stress (σ_y) in colour map, and Figure 2 shows, for each of the applied time integrators, the results over time of σ_y at point B and vertical displacement at point A.

7 Conclusion

The results from section 6 indicate that the choice of parameters for the *alpha*-Generalized method, as well as the time discretization, plays a major role on impact problems. As already discussed in Carvalho [7], Hu's time integrator [18] introduces on the problem a numerical dissipation that is highly dependent to the time discretization, possibly leading to inconsistent results. This can be observed particularly on Figure 2(A), where the Cauchy stress results are shown to be rather unstable when using this time integrator, and discrepant values are found for the two different time discretizations adopted. For the case with $\rho_\infty = 0.6$, we observe similar instabilities on the Cauchy stress results, but the displacement values on Figure 2(B) are higher than the ones obtained with Hu's time integrator after the impact, indicating a less dissipative behaviour, as predicted by the study of Chung and Hulbert [14]. On the other hand, the more dissipative result was found with $\rho_\infty = 0.1$. In this case, the displacement graph shows a response similar to the ones in $\rho_\infty = 0.6$, but the Cauchy stress displays a consistent behaviour when compared to the other cases, despite having a visible damping effect. In conclusion, the *alpha*-Generalized parameters based on the proposal of Chung and Hulbert [14] seem to be more suitable for high-frequency impact problems when compared to the Newmark integrator with Hu's proposed parameters, but a proper identification of the ρ_∞ parameter may be necessary in order to achieve an adequate balance between instability and excessive damping, improving the accuracy of the results.

Acknowledgements. This study was financed in part by the *Coordenação de Aperfeiçoamento de Pessoal de Nível Superior – Brasil* (CAPES) – Finance Code 001 –, the Brazilian agency National Council for Scientific and Technological Development (CNPq) – grant 310482/2016-0 – , and the São Paulo Research Foundation (FAPESP) – Process Number 2018/23957-2. The authors would like to thank them for the financial support given to this research.

Authorship statement. The authors hereby confirm that they are the sole liable persons responsible for the authorship of this work, and that all material that has been herein included as part of the present paper is either the property (and authorship) of the authors, or has the permission of the owners to be included here.

References

[1] T. J. Hughes and E. Carnoy. Nonlinear finite element shell formulation accounting for large membrane strains. *Computer Methods in Applied Mechanics and Engineering*, vol. 39, n. 1, pp. 69 – 82, 1983.

[2] M. Schulz and F. Filippou. Non-linear spatial timoshenko beam element with curvature interpolation. *International Journal for Numerical Methods in Engineering*, vol. 50, pp. 761 – 785, 2001.
[3] M. A. Crisfield. *Nonlinear finite element analysis of solids and structures. Volume 1: Essentials*. Wiley–Blackwell, 1991.
[4] H. B. Coda. An exact fem geometric non-linear analysis of frames based on position description. In *International Congress of Mechanical Engineering*. ABCM, 2003.
[5] R. Carrazedo and H. Coda. Alternative positional fem applied to thermomechanical impact of truss structures. *Finite Elements in Analysis and Design - FINITE ELEM ANAL DESIGN*, vol. 46, pp. 1008–1016, 2010.
[6] H. B. Coda and R. R. Paccola. An alternative positional fem formulation for geometrically non-linear analysis of shells: Curved triangular isoparametric elements. *Computational Mechanics*, vol. 40, n. 1, pp. 185–200, 2007.
[7] P. R. P. Carvalho. Análise numérica bidimensional de sólidos com comportamento visco-elasto-plástico em grandes deformações e situações de contato. Mestrado, Departamento de Engenharia de Estruturas, Escola de Engenharia de São Carlos, Universidade de São Paulo, São Carlos, 2019.
[8] D. H. F. R. Moreira. Análise numérica bidimensional de interação fluido-estrutura com contato estrutural. Mestrado, Departamento de Engenharia de Estruturas, Escola de Engenharia de São Carlos, Universidade de São Paulo, São Carlos, 2021.
[9] G. Avancini and R. A. Sanches. A total lagrangian position-based finite element formulation for free-surface incompressible flows. *Finite Elements in Analysis and Design*, vol. 169, pp. 103348, 2020.
[10] F. Mashayekhi, A. Nobari, and S. Zucca. Hybrid reduction of mistuned bladed disks for nonlinear forced response analysis with dry friction. *International Journal of Non-Linear Mechanics*, vol. 116, pp. 73 – 84, 2019.
[11] T. Hughes, R. Taylor, J. Sackman, A. Curnier, and W. Kanoknukulchai. A finite element method for a class of contact-impact problems. *Computer Methods in Applied Mechanics and Engineering*, vol. 8, pp. 249–276, 1976.
[12] M. A. Puso and T. A. Laursen. A mortar segment-to-segment contact method for large deformation solid mechanics. *Computer Methods in Applied Mechanics and Engineering*, vol. 193, n. 6, pp. 601 – 629, 2004.
[13] P. Wriggers. *Computational Contact Mechanics*. Springer Berlin Heidelberg, 2006.
[14] J. Chung and G. Hulbert. A time integration algorithm for structural dynamics with improved numerical dissipation: The generalized-alpha method. *Journal of Applied Mechanics*, vol. 60, pp. 371–375, 1993.
[15] M. Arnold and O. Bruls. Convergence of the generalized-alpha scheme for constrained mechanical systems. *Multibody System Dynamics*, vol. 18, pp. 185–202, 2007.
[16] T. M. Siqueira. *Ligações deslizantes para análise dinâmica não linear geométrica de estruturas e mecanismos tridimensionais pelo método dos elementos finitos posicional*. Tese de doutorado, Departamento de Engenharia de Estruturas, Escola de Engenharia de São Carlos, Universidade de São Paulo, São Carlos, 2019.
[17] N. M. Newmark. A method of computation for structural dynamics. *Journal of the Engineering Mechanics Division*, vol. 44, pp. 67–94, 1959.
[18] N. Hu. A solution method for dynamic contact problems. *Computers & Structures*, vol. 63, n. 6, pp. 1053 – 1063, 1997.
[19] H. B. Coda. *O Método dos elementos finitos posicional*. EESC/USP, São Carlos, 2018.